

- wide. The thickness was chosen to be 72 nm. Details of the deposition procedure have been described elsewhere [G. Blum, F. Kremer, T. Jaworek, G. Wegner, *Adv. Mater.* **7**, 1017 (1996)].
16. I. Haller, *J. Am. Chem. Soc.* **100**, 8050 (1978).
 17. Kurth and Bein have pointed out that the Haller silanization method results not in a monolayer film but rather in a film of two or three molecular layers due to cross-linking [F. G. Kurth and T. Bein, *Langmuir* **11**, 3061 (1995)]. We have analyzed the coupling layer on Si wafers and quartz slides by small angle x-ray reflection (SAXR) and have consistently found a thickness of 21 ± 3 Å, which agrees with the results of Kurth and Bein. The surface roughness was less than 6 Å.
 18. R. H. Wieringa, E. A. Siesling, A. J. Schouten, in preparation.
 19. Films of comparable thickness grafted on silicon had surface roughnesses of less than 1 nm as determined by SAXR.
 20. Other reflection spectra of grafted PBLG films on various substrates will be published elsewhere. The present spectrum is typical for grafted PBLG films.
 21. The equation used here was derived by F. Mopsik and M. G. Broadhurst [*J. Appl. Phys.* **46**, 4204 (1975)]. It is based on the Onsager approximation of the local field. We are aware of the recent discussion on this approximation [Y. Luo, H. Agren, K. V. Mikkelsen, *Chem. Phys. Lett.* **275**, 145 (1997)]. The polarization given here should, therefore, be treated as a crude estimate.
 22. N. G. McCrum, B. E. Read, G. Williams, *Anelastic and Dielectric Effects in Polymeric Solids* (Dover, New York, 1967).
 23. This estimate is based on the hexagonal packing of PBLG chains with an effective helix radius of 7.7 Å and thus represents a lower limit for the area. Oosterling has recently analyzed PBLG grafted from an aerosol [M. L. C. M. Oosterling, thesis, University of Groningen, Groningen Netherlands (1994)]. His data are consistent with a large area of 460 Å^2 per PBLG chain.
 24. G. Duda et al., *Thin Solid Films* **159**, 221 (1988).
 25. J. Helfrich, R. Hentschke, U. Apel, *Macromolecules* **27**, 472 (1994).
 26. F. Nizzoli et al., *Phys. Rev. B* **40**, 3323 (1989).
 27. E. Fukada, *Ultrasonics* (October 1968), p. 229; L. Jackson, M. T. Shaw, J. H. Aubert, *Polymer* **32**, 221 (1991).
 28. H. Block, *Poly-(γ-Benzyl-L-Glutamate) and Other Glutamic Acid-Containing Polymers* (Gordan & Breach, New York, 1983).
 29. T. Furukawa and J. X. Wen, *Jpn. J. Appl. Phys.* **23**, L677 (1984); J. Naciri, B. R. Ratna, S. Baral-Tosh, P. Keller, R. Shashidhar, *Macromolecules* **28**, 5274 (1995).
 30. G. M. Sessler, in *Topics in Applied Physics*, G. M. Sessler, Ed. (Springer-Verlag, Berlin, 1987), p. 7.
 31. T. Eckert and H. Finkelmann, *Macromol. Rapid Commun.* **17**, 767 (1996).
 32. A. Wada, in *Polyamino Acids, Polypeptides, and Proteins*, M. A. Stahman, Ed. (Univ. of Wisconsin Press, Madison, 1962), p. 131.
 33. We thank G. Glaßer for technical assistance with the Nomarski interferometer and M. L. C. M. Oosterling for fruitful discussions.

15 August 1997; accepted 3 November 1997

Coupling of South American and African Plate Motion and Plate Deformation

Paul G. Silver, Raymond M. Russo, Carolina Lithgow-Bertelloni*

Although the African Plate's northeastward absolute motion slowed abruptly 30 million years ago, the South Atlantic's spreading velocity has remained roughly constant over the past 80 million years, thus requiring a simultaneous westward acceleration of the South American Plate. This plate velocity correlation occurs because the two plates are coupled to general mantle circulation. The deceleration of the African Plate, due to its collision with the Eurasian Plate, diverts mantle flow westward, increasing the net basal driving torque and westward velocity of the South American Plate. One result of South America's higher plate velocity is the increased cordilleran activity along its western edge, beginning at about 30 million years ago.

The motions of tectonic plates are well-established components of plate tectonic theory. Yet, the manner in which plates interact, specifically how the forces driving adjacent plates are coupled to each other, is still uncertain. Plate interaction is most clear at a convergent margin. In a continent-continent collision, the leading edges of both plates are deformed and the velocities of both are constrained to be the same. Subduction represents a more subtle plate interaction, in which the overlying plate is deformed (producing marginal basins or cordilleran structures), although plate velocities are not obviously affected.

Our interest in plate interactions for Atlantic basin plates is motivated by the issue of cordillera formation along the western edge of the American plates, and its rela-

tion to the forces responsible for South American Plate (SA) motion. It was suggested (1, 2) that Andean deformation is a result of the westward velocity of SA and the resistance to that motion by a more slowly retreating subducting Nazca slab. The velocity difference v between the trenchward velocity of the overlying plate and the natural retrograde velocity of the slab determines whether the back arc is under compression (positive) or tension (negative) [for example, (3)]. More generally, a temporal change in v should change the stress state of the back arc. In the case of SA, the onset of the latest phase of Andean deformation, beginning 25 to 30 million years ago (Ma) (4) was concurrent with an increase in the westward velocity of SA (2). A change in plate velocity must be due to a change in the force-balance on the plate. Thus, temporal variations in cordilleran deformation are an expected result of temporal changes in plate driving forces.

To examine this linkage, we analyzed the relative and absolute motion histories of the African Plate (Af) and SA over the last 80 million years (My) using fracture-zone

orientations and sea-floor magnetic anomalies (5), and the motion of Af with respect to Atlantic basin hot spots Tristan da Cunha and St. Helena (6, 7). The variations in SA and Af velocity vectors were determined from the stage poles of motion that were decomposed, as angular velocity vectors, into directions parallel and orthogonal to the relative plate motion direction (defined as the 80 My finite rotation pole). The corresponding plate directions are roughly east-west and north-south, respectively. While the half-spreading rate between the Af and SA remained relatively constant at 2 cm/year over the last 80 My, the absolute motion of Af slowed considerably beginning at about 30 Ma. Af's eastward velocity before this time averaged about 2.5 cm/year, but subsequently dropped to 1 cm/year (Fig. 1) (8). The combination of a roughly constant relative velocity and an abrupt reduction in Af's eastward velocity, requires a simultaneous increase in the absolute westward velocity of SA. During the last 30 My, this velocity increased from about 2.0 to 2.8 cm/year (Fig. 1). SA is currently moving faster relative to the hot spots than at any time in the last 80 My.

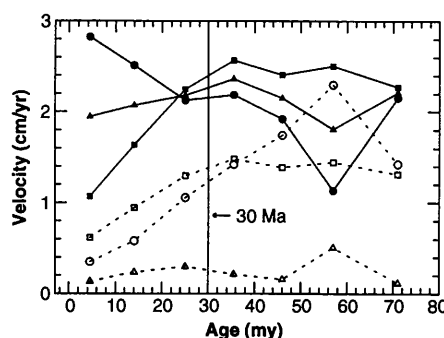
A simple explanation for the deceleration of Af is its collision with the Eurasian Plate (Eu), beginning about 38 Ma [for example, (9, 10)], which is the largest and slowest moving plate (11, 12). The simultaneous westward acceleration of SA, however, requires a separate mechanism. We propose that the change in SA's motion is the result of a flow-coupled plate interaction. If Af and SA are coupled to mantle flow (13), a change in Af motion perturbs the mantle flow field, which in turn alters the basal shear stress and, hence, the velocity of SA. The existence of this interaction is independent of whether the plates drive the flow or vice

P. G. Silver and C. Lithgow-Bertelloni, Department of Terrestrial Magnetism, Carnegie Institution of Washington, 5241 Broad Branch Road, N.W., Washington, DC 20015, USA.

R. M. Russo, Department of Geological Sciences, Northwestern University, Evanston, IL 60208, USA.

*Present address: Department of Geological Sciences, University of Michigan, Ann Arbor, MI, 48109, USA.

Fig. 1. SA (circles) and Af (squares) absolute velocities and SA/Af relative velocities (half-spreading rate) (triangles) for the last 80 My corresponding to the stage poles calculated from plate motion models. Each stage pole is treated as an angular velocity vector and is decomposed into components that are parallel (solid lines, filled symbols) and orthogonal (dashed lines, open symbols) to relative plate motion pole, defined as the 0 to 80 Ma finite rotation pole for relative motion. The two component directions of motion are approximately east-west and north-south, respectively. Velocities are plotted at the middle of the time interval for which they are calculated and given as velocity at the equator of the plate. For east-west motion, note that SA/Af relative motion has a roughly constant half spreading velocity of about 2 cm/year. In contrast, Af absolute motion slows abruptly after 30 Ma (vertical line), going from a value of about 2.5 cm/year before 30 Ma to about 1 cm/year at present. SA increases in velocity from about 2 cm/year up to a present value of 2.8 cm/year. North-south velocities for the two plates both decrease at about the same rate from 30 Ma to the present. The apparent correlation of SA and Af absolute motion indicate two forms of plate interactions: a flow-coupled plate interaction (east-west motions) and a ridge-transform plate interaction (north-south motions, see text).



versa. In the former case, if the dominant driving force is, for example, lithospheric cooling or ridge-push, basal shear is a drag force on the plate. The eastward flow that is induced by Af motion ceases when the plate stops. There is, then, a net westward flow that serves to reduce the drag force beneath SA. The resulting divergence velocity remains unchanged (14).

If the plates are driven by general mantle circulation, basal shear is a driving force. The eastward motion of the mantle beneath Af is impeded if that plate stops, in which case mantle circulation is diverted westward, increasing the net basal driving torque on SA. A constant divergence velocity will arise if there is a constant mass flux of material entering the Atlantic

basin mantle.

As a test of the plausibility of this flow-coupled mechanism, we performed a three-dimensional instantaneous flow calculation in which mantle flow is assumed to be driven by two known sources of buoyancy: The density anomalies produced by slabs subducted over the last 200 My and lithospheric cooling (15). To approximate the effect of a collision between Af and Eu on the mantle flow field, and on the velocity of adjacent plates, we compared two cases at 25 Ma: one in which the velocities of Af and Eu were independent (pre-collision), and one in which they were constrained to have the same velocity (post-collision) (16, 17). The difference between pre- and post-collision plate velocities (Fig. 2), reflecting a flow-coupled plate interaction, was significant for plates adjacent to Af. For SA, there was an added southwesterly component of plate motion; the magnitude of this motion near the western edge of SA was 0.5 to 1.0 cm/year (~25% change in velocity), similar to the change found in the actual plate motion.

This flow-coupled plate interaction, in addition to linking plate velocities, links stress changes and accompanying deformation as well. The Af-Eu collision increased the resistive force that Eu exerted on Af and gave rise to deformation along the western

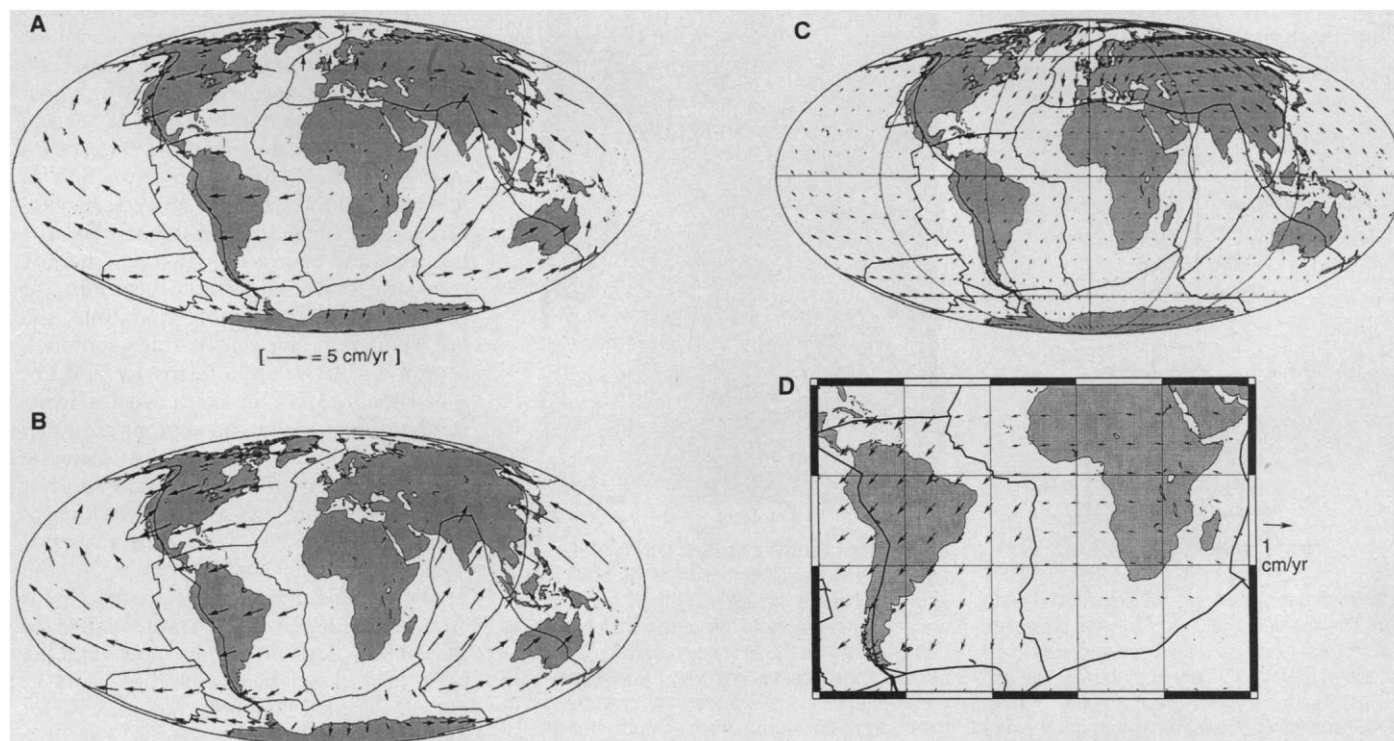


Fig. 2. Test of flow-coupled plate interaction hypothesis. Instantaneous flow calculation to predict plate motion for the 25 to 43 Ma stage using sources of buoyancy due to density anomalies associated with subduction over the preceding 200 My and lithospheric cooling (15). (A) plate motion (no-net-torque reference frame) with Af and Eu as separate plates (pre-collisional); (B) same as (A), but with Af and Eu acting as one plate with the

same velocity (post-collisional). (C) Difference between pre- and post-collisional plate motion vectors. (D) Close-up of differential velocity vectors between Af and SA from (C). Note that Af has essentially stopped and SA possesses a southwesterly change in plate motion of almost 1 cm/year. The westward component is predicted by the flow-coupled plate interaction hypothesis.

part of the Alpine-Himalayan chain. The corresponding westward acceleration of SA increased the resistive normal stress, and consequent cordillera deformation, on that continent's western leading edge. As noted above, this change in motion is temporally related to Altiplano and Bolivian orocline formation during the latest phase of Andean deformation, as well as the onset of eastward motion of the Caribbean Plate, and opening of the Drake Passage south of Patagonia (2). Thus, Andean and Alpine-Himalayan deformation are causally linked by this flow-coupled plate interaction.

Assuming that SA's increase in trenchward velocity since 30 Ma, defined as $\delta v(t)$, is taken up entirely by east-west shortening, it is possible to predict the amount of cordilleran shortening from plate motion by integrating $\delta v(t)$ from 30 Ma to the present. The resulting 120 km estimate for total shortening (based on the average 0.4 cm/year increase in SA velocity since 30 Ma) is comparable to the actual shortening inferred to have occurred throughout the central Andes over this time period (18). In addition, the present-day value of $\delta v(t) = 0.8$ cm/year (Fig. 1) is close to the present-day rate of shortening across the Andes of about 1 cm/year, estimated from Global Positioning System (GPS) measurements taken on either side of the Andes (19).

The motions of SA and Af reveal a

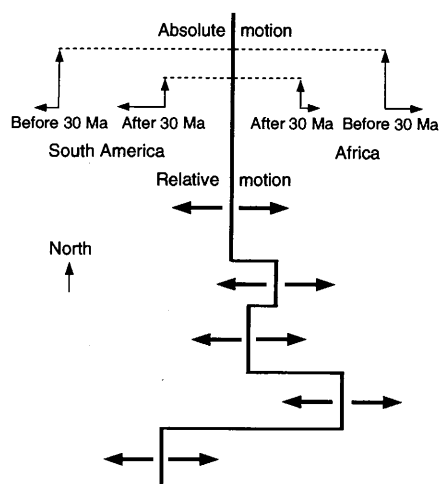


Fig. 3. Schematic of a ridge-transform plate interaction. The absolute motions of the two plates are shown for the northward (vertical) and east-west (horizontal) directions before and after 30 Ma. Absolute motions in the (northward) direction orthogonal to the east-west relative plate motion direction are constrained to be the same for the two plates. If this were not the case, then the ridge-transform offsets (connected solid lines) would have to be broken and the ridge completely reorganized. Thus, the deceleration of Af's northward motion at about 30 Ma (Fig. 1) required a simultaneous deceleration in SA's northward motion.

second type of coupling, signaled by the simultaneous reduction in the two plates' northward motions since 30 Ma (Fig. 1). We infer that the coupled motion is due to the plate strength and structure of transform faults at the Mid-Atlantic Ridge (MAR) (20). The onset of differential Af and SA north-south motion at 30 Ma would have required a reorganization of the interlocking MAR-transform system (Fig. 3). New transform faults trending parallel to the new relative plate motion directions would have had to break through already formed oceanic lithosphere of both plates to accommodate such a change in motion. Thus, SA absolute motion is severely restricted in the direction orthogonal to relative plate motion.

The strength of the ridge-transform system can be used as an upper bound on the northward driving forces on SA because

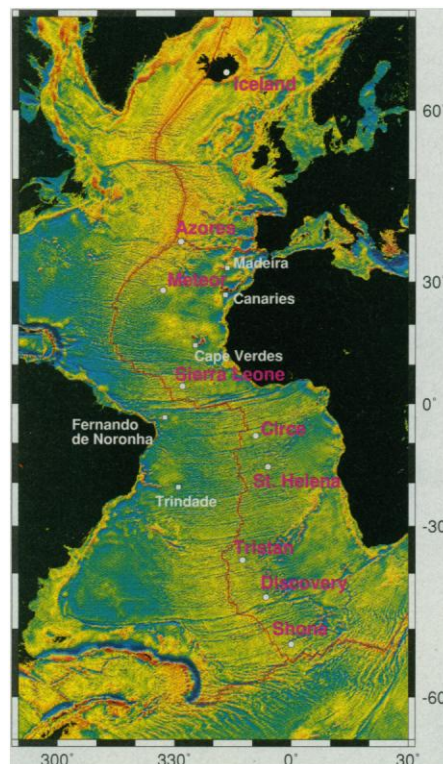


Fig. 4. Map of sea-floor bathymetry for the Atlantic basin (31), along with location of the MAR and of known hot spots (circles) and other centers of volcanism (squares). Note the large transform offsets that characterize the Atlantic spreading center, especially those associated with the west African continental bulge. It is argued that the strength of these ridge-transform offsets couple the north-south velocities of the Af and SA plates. Also note that all of the Atlantic basin hot spots are to the east of the ridge, suggesting a general westward shift in the center of mass of the Atlantic basin in a hot-spot frame. Based on the timing of the shift at Iceland, we infer that NA absolute motion accelerated to the west at the same time as SA.

the two forces must balance. The strength of this system depends on its evolution over the last 130 My and is primarily a function of the geometry of Mesozoic continental breakup. The force required to break oceanic lithosphere under shear is roughly a linear function of age and is about 5×10^{-12} N/m of ridge for 30-My lithosphere (21). This estimate is appropriate for the southern part of the ridge, but the ridge-transform strength must be greater to the north, where long ridge-offsets accommodate the west African continental bulge (Fig. 4). Assuming that the northern region is twice as strong, the average resistive force is closer to 7.5×10^{-12} N/m, which then represents an upper bound on the basal traction driving SA northward (22).

On the basis of our analysis of SA-Af motions, we expect a westward acceleration of the North American Plate (NA) that is comparable to that for SA. If this were not the case, east-west differential motion between NA and SA should be evident (most probably east of the Caribbean Plate) beginning about 30 Ma, and there is no evidence for such differential motion (23). Available hot-spot data for NA are consistent with this hypothesis. Late Cenozoic westward drift of the MAR system, relative to proximal hot spots, has generally occurred throughout the Atlantic basin (24, 25) (Fig. 4). The history of such motion in the North Atlantic is best revealed by motion of the MAR relative to the Iceland hot spot. Age dating and geochemical analyses of hot-spot lavas and ridge lavas indicate progressive westward motion of the MAR north and south of Iceland, and formation of an eastern, captured ridge segment coincident with the hot spot, and bounded by two lengthening transform faults, detectable beginning at about 30 Ma (26). Before that time, the hot spot was apparently ridge-centered. Motion of NA relative to the Iceland hot spot therefore is consistent with a westward acceleration at the appropriate time.

The apparent relationship between the MAR and many of the Atlantic basin hot spots (Fig. 4) suggests westward motion of the entire MAR in a hot-spot reference frame. Like the Iceland hot spot, the Tristan da Cunha hot spot in the South Atlantic is displaced eastward relative to the MAR. Both hot spots now underlie crust formed at the time of anomaly 6, around 20 Ma. Similarly, the Azores hot spot (25, 27–29) also lies some 200 km east of the adjacent MAR, as do nearly all of the other proposed Atlantic hot spots (30).

Flow-coupled plate interactions illustrate the importance of the mantle flow field in controlling plate motion and tectonic activity. They are a natural conse-

quence of continent-continent collisions between large plates that are strongly coupled to mantle flow, and may thus provide a means of linking major tectonic events that have occurred throughout Earth's geologic history.

REFERENCES AND NOTES

1. R. M. Russo and P. G. Silver, *Science* **263**, 1105 (1994).
2. ———, *Geology* **24**, 511 (1996).
3. S. Uyeda and H. Kanamori, *J. Geophys. Res.* **84**, 1049 (1979).
4. T. Sempere *et al.*, *Geology* **18**, 946 (1990).
5. P. Shaw and S. C. Cande, *J. Geophys. Res.* **95**, 2625 (1990).
6. J. M. O'Connor and R. A. Duncan, *ibid.*, p. 17475.
7. J. M. O'Connor and A. P. le Roex, *Earth Planet. Sci. Lett.* **113**, 343 (1992).
8. Supporting evidence for this reduction in the Af velocity was summarized by K. Burke [S. Afr. J. Geol. **99**, 341 (1996)].
9. K. J. Hsu, *Geol. Soc. Am. Spec. Pub.* **45**, 421 (1989).
10. J. Dercourt, L. E. Ricou, B. Vrielynck, Eds., *Atlas Tethys Paleoenvironmental Maps* (Gauthier-Villars, Paris, 1993).
11. A. E. Gripp and R. G. Gordon, *Geophys. Res. Lett.* **17**, 1109 (1990).
12. P. R. Stoddard and D. Abbott, *J. Geophys. Res.* **101**, 5425 (1996).
13. There are several lines of evidence supporting the notion that SA is coupled to general mantle circulation. First, the only other potentially significant driving force, ridge-push, does not change on sufficiently short time scales to cause such a rapid change in plate motion. The change must be caused by changes in the tractions at the plate boundary or basal tractions. There is no evidence for a decrease in boundary resistance forces or increase in boundary driving forces, so the only alternative is a change in the basal traction (that could take the form of basal shear tractions or possibly horizontal normal tractions applied to the sides of deep continental roots). Other lines of evidence include: the apparent absence of an asthenospheric decoupling zone beneath continental plates in general [P. G. Silver, *Annu. Rev. Earth Planet. Sci.* **24**, 385 (1996)] and South America in particular [D. E. James and M. Assumpção, *Geophys. J. Int.* **126**, 1 (1996)], as inferred from seismic anisotropy, and the suggestion, from seismic tomography of coherent translation of the SA plate and upper mantle over the last 130 My [J. C. Van Decar, D. E. James, M. Assumpção, *Nature* **378**, 25 (1995)]. If SA is coupled to mantle circulation, it is reasonable to suppose that the other plates of the Atlantic basin, particularly Africa, are similarly coupled (2). For a general discussion of coupling of plate motions to mantle circulation, see C. Lithgow-Bertelloni and M. A. Richards, *Rev. Geophys.*, in press.
14. It is unlikely for there to be any other way for stress to be transmitted from Af to SA. If transmitted through the plates themselves (acting as a stress guide), the stress would have to cross the ridge, where plates are thinnest, leading to a severe disruption in the spreading process, which is not observed.
15. C. Lithgow-Bertelloni and M. A. Richards, *Geophys. Res. Lett.* **22**, 1317 (1995). We used a density heterogeneity model based on the 200 My of subduction preceding 25 Ma and on oceanic lithospheric ages consistent with the plate boundaries and age of the stage. The viscosity structure used in the calculation (a lower mantle 50 times more viscous than the upper mantle) represents the value obtained from a fit to the geoid, assuming a present-day density heterogeneity field based on subduction history. The absolute viscosity was fixed at 10^{21} Pas, a value compatible with inferences from post-glacial rebound.
16. By allowing Af and Eu to act as one plate, we are implicitly allowing infinite compressional stresses to develop at the plate boundary between them, maximizing the effect of the collision. The size of the colliding plates is crucial for the collision to have any effect on the general mantle circulation. This approach was attempted previously (17) as a way of testing the influence of the India/Eurasia collision on the Pacific Plate, although no change in plate motion was found.
17. M. Richards and C. Lithgow-Bertelloni, *Earth Planet. Sci. Lett.* **137**, 19 (1996).
18. These are estimated from balanced cross sections, which range from 100 to 200 km: F. Megard, *J. Geol. Soc. London* **129**, 893 (1984); B. M. Sheffels, *Geology* **18**, 812 (1990); R. W. Allmendinger *et al.*, *Tectonics* **2**, 1 (1983); R. W. Allmendinger *et al.*, *ibid.* **9**, 789 (1990); P. Baby *et al.*, *ibid.* **11**, 523 (1992).
19. L. Leffler *et al.*, *Geophys. Res. Lett.*, **24**, 1031 (1997); E. Norabuena *et al.*, *Science*, in press.
20. Described by M. A. Richards and D. C. Engebretson [*Eos Trans. Am. Geophys. Union* **75**, 63 (1994)] for Pacific-Farallon motions at the time of the formation of the bend in the Hawaii-Emperor sea mount chain. S. Zhong and M. Gurnis [*Nature* **383**, 245 (1996)] showed that transforms guide plate motions in mantle convection models with realistic faults and plates.
21. J. Mammertickx and D. Sandwell, *J. Geophys. Res.* **91**, 1975 (1986).
22. This estimate is based on the assumption that SA's northward motion is primarily driven by basal shear and that the ridge-transform offsets have become the dominant resistive force once SA's northward motion has ceased.
23. T. H. Dixon and A. Mao, *Geophys. Res. Lett.* **24**, 535 (1997).
24. S. Stein, H. J. Melosh, J. B. Minster, *Earth Planet. Sci. Lett.* **36**, 51 (1977).
25. J. G. Schilling, *Nature* **352**, 397 (1991).
26. N. Oskarsson, S. Steinthorsson, G. E. Sigvaldason, *J. Geophys. Res.* **90**, 10011 (1985).
27. W. J. Morgan, *Am. Assoc. Pet. Geol. Bull.* **56**, 203 (1972).
28. J. Madeira and A. Ribeiro, *Tectonophysics* **184**, 405 (1990).
29. E. Widom, R. W. Carlson, J. B. Gill, H. U. Schminke, *Chem. Geol.*, in preparation.
30. The New England hot spot in the Great Meteor-Atlantis seamounts [R. A. Duncan, *J. Geophys. Res.* **89**, 9980 (1984); B. E. Tucholke and N. C. Smoot, *ibid.* **95**, 17555 (1990)], which also lie a few hundred kilometers east of the adjacent MAR. Further south, isotopically distinct Sierra Leone, Circe, Shona, and Discovery mantle plumes have been observed in a similar eastward-displaced position relative to the local MAR [C. J. H. Hartnady and A. P. le Roex, *Earth Planet. Sci. Lett.* **75** (1985); J. G. Schilling *et al.*, *J. Geophys. Res.* **99**, 12005 (1994); J. Douglass, J. G. Schilling, R. H. Kingsley, C. Small, *Geophys. Res. Lett.* **22**, 2893 (1995)]. Although the motion histories of these hot spots are poorly known compared to that of Iceland or Tristan da Cunha, the regular distribution of near-MAR hot spots on the east side of the ridge is compatible with westward drift of the MAR relative to Atlantic basin hot spots since at least 30 Ma.
31. D. T. Sandwell and W. H. F. Smith, *J. Geophys. Res.*, in press.
32. We thank W. Smith for providing us with a custom version of Atlantic basin gravity anomalies; S. Solomon, C. DeLima, S. Stein, P. Lundgren, C. Bina, A. Nicolas, and A. le Roex for stimulating discussions; S. Sacks for South American GPS data before publication; J. Dunlap for manuscript preparation; and M. Acierio and S. Keiser for computer support. We used GMT (P. Wessel and W. Smith) to make many figures in this report. Supported by NSF grant EAR 93-16457 (P.G.S. and R.R.), by an NSF-NATO Fellowship (R.R.), by an NSF postdoctoral fellowship (C.L.-B.) and by the Carnegie Institution of Washington (P.G.S. and C.L.-B.).

3 February 1997; accepted 24 November 1997

Footwall Refrigeration Along a Detachment Fault: Implications for the Thermal Evolution of Core Complexes

Jean Morrison* and J. Lawford Anderson

Oxygen isotope compositions of epidote and quartz from chloritic breccias that underlie the detachment fault in the metamorphic core complex of the Whipple Mountains yielded quartz-epidote fractionations that range from 4.1 to 6.4 per mil and increase systematically toward the fault. These fractionations give mean temperatures that decrease from $\sim 432^\circ\text{C}$ at 50 meters below the fault to $\sim 350^\circ\text{C}$ at 12 meters below the fault. This extreme thermal gradient of 82°C over 38 meters (2160°C per kilometer) is best explained by advective heat extraction by means of circulating surface-derived fluids. Models of lithospheric extension consider only conductive cooling resulting from tectonic denudation and thus require revision to include fluid-induced fault-zone refrigeration.

Metamorphic core complexes of the western North American cordillera formed during pronounced Cenozoic crustal extension at the lithospheric scale. Core complexes are characterized by regionally extensive, low-angle detachment faults that accom-

modate large, lateral displacements of the crust (1–3). An accurate and quantitative understanding of the nature of movement along detachment faults is essential in developing realistic models of lithospheric extension. However, many aspects of detachment fault systems, including the determination of whether they initiate and slip at low angles ($<30^\circ$), the rates at which they slip, and the role that fluids play in the

Department of Earth Sciences, University of Southern California, Los Angeles, CA 90089-0740, USA.

*To whom correspondence should be addressed.